Pharm Res (2014) 31:1275–1289
DOI 10.1007/s11095-013-1249-3

RESEARCH PAPER

Mono and Dually Decorated Nanoliposomes for Brain Targeting, *In Vitro* and *In Vivo* Studies

E. Markoutsa • K. Papadia • A. D. Giannou • M. Spella • A. Cagnotto • M. Salmona • G. T. Stathopoulos • S. G. Antimisiaris

Received: 16 July 2013 / Accepted: 10 November 2013 / Published online: 13 December 2013

ABSTRACT

Purpose Mono- and dual-decorated (DUAL) liposomes (LIP) were prepared, by immobilization of MAb against transferrin (TfR[OX26 or RI7217]) and/or a peptide analogue of ApoE3 (APOe) -to target low-density lipoprotein receptor(LPR)-, characterized physicochemically and investigated for BBB-targeting, *in-vitro* and *in-vivo*.

Methods Human microvascular endothelial cells (hCMEC/D3) were used as BBB model, and brain targeting was studied by *in-vivo* imaging of DiR-labelled formulations (at two doses and surface ligand densities), followed by *ex-vivo* organ imaging.

Results LIP diameter was between 100 nm and 150 nm, their stability was good and they were non-cytotoxic. LIP uptake and transport across the hCMEC/D3 cell monolayer was significantly affected by decoration with APOe or MAb, the DUAL exerting an additive effect. Intact vesicle-transcytosis was confirmed by equal transport of hydrophilic and lipophilic labels. *In-vivo* and *ex-vivo* results confirmed MAb and DUAL-LIP increased brain targeting compared to non-targeted PEG-LIPs, but not for APOe (also targeting ability of DUAL-LIP was not higher than MAb-LIP). The contradiction between *in-vitro* and *in-vivo* results was overruled when *in-vitro* studies (uptake and monolayer transport) were carried out in presence of serum proteins, revealing their important role in targeted-nanoformulation performance.

Conclusions A peptide analogue of ApoE3 was found to target BBB and increase the targeting potential of TfR-MAb decorated LIP, *in-vitro*, but not *in-vivo*, indicating that different types of ligands (small peptides and antibodies) are affected differently by *in-vivo* applying conditions. *In-vitro* tests, carried out in presence of serum proteins, may be a helpful predictive "targetability" tool.

KEYWORDS brain · ligand · liposomes · live-animal imaging · nanoparticle · proteins · serum · targeting

INTRODUCTION

The blood–brain barrier (BBB) protects neurons and preserves the CNS but prevents many drugs to reach the brain (1), generating the largest problems for therapy of brain-located pathologies. Several non-invasive approaches have been proposed to overcome this barrier, as development of targeting carrier systems which can be endocytosed by brain endothelial cells *via* receptors they overexpress. Such methodologies have been successful for targeted delivery of anticancer drugs to cancer cells (2–7) or delivery of higher amounts of drugs (compared to those delivered as free drug) to the brain (8–11). Drugs loaded in such systems may be delivered to the brain, providing that their association with the carrier is stable during the journey from the site of administration to the site of interest. Between drug delivery systems (DDSs), liposomes (LIPs) have many advantages (12,13) (as increased drug capacity, versatile structure and facile surface decoration,

Electronic supplementary material The online version of this article (doi:10.1007/s11095-013-1249-3) contains supplementary material, which is available to authorized users.

E. Markoutsa • K. Papadia • S. G. Antimisiaris (✉)
Laboratory of Pharmaceutical Technology, Department of Pharmacy
University of Patras, Rio, Patras 26510, Greece
e-mail: santimis@upatras.gr

A. D. Giannou • M. Spella • G. T. Stathopoulos
Laboratory for Molecular Respiratory Carcinogenesis
Department of Physiology, Faculty of Medicine, University of Patras
Rio, Patras 26510, Greece

A. Cagnotto • M. Salmona
Department of Biochemistry and Molecular Pharmacology
IRCCS-Istituto di Ricerche Farmacologiche "Mario Negri", Milan, Italy

S. G. Antimisiaris
Foundation for Research and Technology, Hellas
Institute of Chemical Engineering Sciences, FORTH/ICES
Rio, Patras 26504, Greece

biocompatibility, biodegradability, minimum toxicity, *etc.*) while the ability to label both their lipid and aqueous compartments, permits accurate exploitation of cell-vesicle interactions (14), and vesicle biodistribution (15,16). Multiligand-decorated LIPs, are more efficient (compared to LIPs with one ligand) to target specific diseases or cells (16–21); especially when more than one receptors (or epitopes of the same receptor) are targeted (22). With the aim to develop brain-targeted liposomes for delivery of imaging and/or therapeutic agents against Alzheimers disease (AD)-related-pathologies, mono-ligand decorated LIPs (MONO) and dual-ligand decorated LIPs (DUAL) were prepared, using an anti-transferrin monoclonal antibody (MAb) (known to target TfR) (14,23–26) and a peptide derivative of apolipoprotein E3 (APOe) to target the low-density lipoprotein receptor related protein (LPR), for the first time together on the same LIP. In order to investigate if DUAL LIPs have increased BBB targeting capability compared to the corresponding MONO ones, *in vitro* and *in vivo* experiments were performed, in which the targeting capability of the different LIP types was compared with non-tagreted, PEG-LIPs. The APOe peptide used herein was recently demonstrated to increase the interaction of liposomes with BBB-cellular models, when immobilized on their surface (compared to liposomes with no peptide) (27,28), however the *in vivo* performance of APOe-LIPs as BBB targeting nanotechnologies is tested for the first time. After applying different ligand attachment methodologies, in order to achieve optimal ligand attachment and LIP recovery yields, MONO and DUAL LIPs were evaluated under identical experimental conditions for their brain targeting potential; first on a cellular model of BBB (*in-vitro*) and after that, *in-vivo* (by live animal imaging in wild type mice) in order to investigate if the *in vitro* model of the BBB can predict *in vivo* performance (29). hCMEC/D3 cells, which have been demonstrated to form junction complexes (30) and be reliable for screening drugs (31) and targeted LIPs (14,25,32,33) for their BBB transport capability, were used.

MATERIALS AND METHODS

1,2-distearoyl-sn-glycerol-3-phosphatidylcholine (DSPC), 1,2-distearoyl-sn-glycerol-3-phosphoethanolamine-N-[methoxy(polyethyleneglycol)-2000] (DSPE-PEG_{2000} [PEG-lipid]), 1,2-distearoyl-sn-glycerol-3-phosphoethanolamine-N-[biotinyl (polyethyleneglycol) -2000] [PEG-Biotin], 1,2-distearoyl-sn-glycero-3-phosphoethanolamine-N-[maleimide(polyethylene glycol)-2000] [PEG-Mal] and lissamine rhodamine B phosphatidylethanolamine [RHO-lipid] were purchased from Avanti Polar Lipids. Fluorescein-isothiocyanate-dextran-4000 [FITC], streptavidin from *S. avidinii* [STREP], lucifer yellow-CH dilithium salt (LY), 10 nm gold nanoparticle labeled rabbit anti-mouse antibodies, Sephadex G-50 and Sepharose CL-4B, were from Sigma-Aldrich. Mouse anti-rat CD71 IgG2a (clone OX-26 [for *in vitro* studies]) was obtained from Serotec and anti-mouse CD71 IgG2a (clone RI7217 [for *in vivo* studies]) was from Biolegend. Amicon-Ultra 15 tubes (Millipore) were used for sample concentration. Protein concentrations were measured, by Bradford microassay (Biorad). Antibodies were biotinylated using the EZ-link Biotinylation kit (Pierce), as reported (14). MAb thiolation was performed by the Traut's reagent (Pierce); For this, the MAb solution (1 mg/ml, 1 ml) was first concentrated to 100 μl with Amicon Ultra-15 Centrifugal Filter Devices (10 kDa cut off) and then mixed with 900 μl degassed Borate buffer containing 36 μl of 1 mg/ml Traut's reagent. The reaction was carried out for 1.5 h in the dark, at room temperature and under N_2 and continuous stirring. The non-reacted Trauts reagent was isolated after 3 washes with PBS using Ultra-15 Centrifugal Filter Devices (Amicon). Quantification of sulfhydryl (SH) groups was performed by the Ellman's reagent (Sigma), to calculate the thiolation yield. Lipophilic tracer 1,1-dioctadecyl-3,3,3,3-tetramethylindotricarbocyanine iodide (DiR; Molecular Probes) was used as liposome label for live animal imaging.

Fluorescence intensity (FI) was measured by Shimatzu RF-1501 spectrofluorometer. Conditions used: (i) For Rho-lipid: EX-550 nm/EM-575 nm; (ii) For FITC: EX-490 nm/EM-525 nm. In all cases 5 nm slits were used. A bath sonicator (Branson) and microtip-probe sonicator (Sonics and Materials) were used for liposome preparation.

Synthesis and Characterization of APOe Peptides

The sequence of aminoacid residues 141–150 of human APOe peptide and its tandem dimer repeat (141–150) were synthesized by automated peptide synthesizer (Applied Biosystems) at 0.1 mM scale. A NOVASYN-TGA resin (Novabiochem) was used, with Fmoc-protected l-amino acid4s (Flamma). Peptides were bearing a tryptophan residue at C-terminal (which was utilized for fluorescence detection) and ended with a cysteine residue, utilized for covalent coupling with PEG-Mal. Amino acids (AA) were activated by reaction with O- 101 (Benzotriazol-1-yl)-N,N,N,N-tetramethyluronium tetrafluorobo- rate and N,N-diisopropylethylamine. A capping step with acetic anhydride after the last coupling cycle of each AA was included. Peptides were cleaved from resin with trifluoroacetic acid:thioanisole:water:phenol:ethanedithiol (82.5:5:5:2.5, v/v), precipitated and washed with diethyl ether. Precipitate was purified by RP- HPLC on semi-preparative C4 column (Symmetry 300, Waters) and peaks were characterized by matrix-assisted laser desorption/ionization (MALDI) mass spectrometry. Peptide purity (>95%) was assessed by HPLC

and MALDI . Fractions containing purified peptides were lyophilized and stored at −20°C.

Liposome Preparation

LIPs were prepared by thin film hydration followed by probe sonication, as previously described (14,25). Hydration was performed by PBS, pH 7.40, or 36 mM FITC-dextran or 100 mM calcein (osmolarity adjusted to 300 mOsm). In some cases, vesicles were additionally labeled with RHO-lipid or only with DiR (both added in the lipid mixture). After initial formation of liposome dispersions, size was reduced by probe sonication (Sonics & Materials). Free FITC-dextran and/or non-incorporated dye was separated from liposomes by Sepharose 4B-CL (1×35 cm) column, or by ultracentrifugation (40 min at 40.000 rpm, Sorvall WX90 Ultra, Thermo Scientific).

In addition to DUAL (decorated with MAb plus APOe (monomer or dimer)) the other LIP types were: (i) Pegylated liposomes (PEG-LIP), as control vesicles, consisting of DSPC/Chol/PEG-lipid at 20:10:1.6 (mole/mole); (ii) MONO with MAb (MAb-LIP); (iii) MONO with APOe (APOe-LIP). A schematic diagram of the various LIP types prepared including stepwise representation of the reactions carried out is provided (Scheme 1). Details about compositions and attachment methodologies follow.

Immunoliposomes (MAb-LIPs)

Pre-formed LIPs with surface biotin or MAL- groups, consisting of DSPC/Chol/PEG-lipid/PEG-Biotin or PEG-MAL at 20:10:1.6:0.01 (mole ratios), were prepared, as described above, and MAb attachment was performed by the biotin/STREP/biotin ligand attachment methodology, as reported recently (14,25), or by MAL-thioether reaction. In the last case PEG-MAL containing LIPs were mixed with thiolated -MAb (the thiolation was performed as presented above) and incubated at room temperature for 4 h, and then at 4°C overnight. Non-attached antibody was removed by gel filtration (Sepharose 4B-CL) and collected for antibody attachment yield calculation (performed by an Elisa technique as previously described (14,25)). The MAb attachment yield was similar for both methodologies used ranging between 60 and 85%.

APOe-LIPs

Pre-formed PEG-MAL containing LIPs, consisting of DSPC:Chol:PEG-lipid:PEG-MAL at 20:10:1.6:0.01 (mole ratios), and control liposomes (without PEG-Mal) were prepared, as above. For APOe conjugation by thioether bond between the peptide cysteine and the MAL-groups of the vesicles, LIPs were incubated overnight with peptide (at 1.1 M excess) at 25°C, and their FI was measured (EX-280 nm, EM-350 nm) before and after purification from non-attached peptide by extensive dialysis. Non-specific binding of APOe was calculated by using control liposomes (with no MAL-groups), under identical conditions. Peptide attachment yield was calculated from initial and final FI (by comparing FI/mol lipid). (Supplementary Material).

When low PEG-lipid amounts were used in LIPs, peptide attachment yield was very low, practically equal to non-specific binding, most possibly due to inability of peptides to approach MAL-groups hidden within PEG chains in

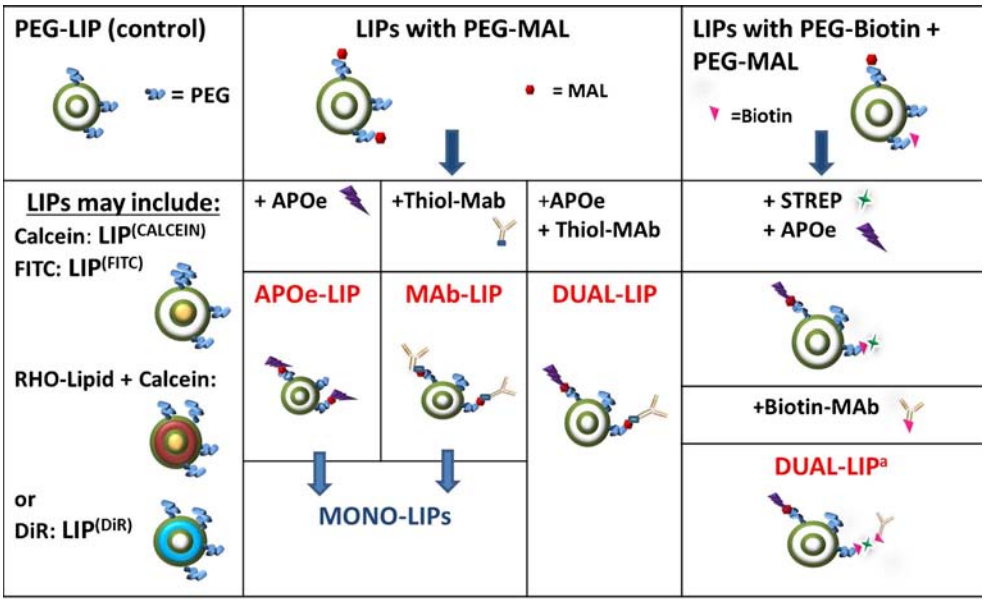

Scheme 1 Schematic representation of the various types of constructed LIPs, and simple stepwise presentation of preparation methodologies. For more details of methodologies see Materials and Methods section and Supplementary Material

[a]: This type of DUAL-LIP was constructed but not used for in vitro/in vivo testing due to low lipid recovery.

"mushroom" conformation (33). However, it increased to practically 100% when higher amounts of PEG-lipid were used (Supplementary Material). Since the pH was not found to have an effect on the peptide attachment yield (in the range studied, a pH of 7.40 was routinely used for peptide attachment (Supplementary Material).

DUAL-LIPs

LIPs with surface -MAL groups, consisting of DSPC/Chol/PEG-lipid/PEG-Mal at 20:10:1.6:0.01 (or 0.02) (mole ratios) were prepared and APOe mixed with thiolated -MAb (the thiolation was performed by Traut's reagent as presented above) were incubated with the LIPs at room temperature for 4 h, and then at 4°C overnight. LIP purification (from non-attached ligands) and APOe/MAb attachment yield measurements, were performed, as described above. Initially, the immobilization of the two ligands was performed by the two different ligation methodologies (Supplementary Material), but finally the ligation *via* MAL groups (after thiolation of the MAb) was preferred due to simplicity, increased LIP lipid yield (the number of steps of the procedure were significantly reduced, and so was the overall loss of lipid) and similar attachment yield. With the last attachment protocol the attachment yield in DUAL-LIPs was between 60% and 73% for the MAb, and between 78 and 95% for APOe. The slight reduction in APOe attachment yield is attributed to the competition between the peptide and the MAb for the same MAL groups of the pre-formed liposomes. Since the same ligation was selected for both ligands in the DUAL LIPs, the MAL-thiol ligation was also used for all the MAb-LIPs evaluated *in vitro* and *in vivo*.

Liposome Physicochemical Characterization

Vesicle Entrapment Efficiency

The dye/lipid (mol/mol) ratio was measured in order to calculate the amount of lipid from corresponding dye concentration. The lipid concentration was measured by Stewart assay (34).

Size Distribution and Zeta Potential Measurements

Particle size of vesicle dispersions (0.4 mg/ml) was measured by dynamic light scattering (DLS) (Malvern Nano-Zs, Malvern Instrument, UK) at 25°C and 173° angle. Zeta Potential was measured (dispersed in 10 mM PBS, pH 7.40) at 25°C, utilizing the Doppler electrophoresis technique.

LIP Integrity

The integrity of LIPs was studied by measuring retention of LIP-entrapped calcein [100 mM] or FITC-dextran, during incubation in absence/presence of serum proteins or cell culture medium. Calcein latency and retention was calculated, as reported (35). For FITC-dextran, LIPs were separated from free FITC-dextran by gel filtration, before dye leakage was calculated. No quenching of FITC-dextran was detected at the concentrations used.

Transmission Electron Microscopy (TEM)

LIPs (1–2 mg/ml) were deposited on formvar-coated carbon reinforced 300 mesh copper grids (Agar Scientific, Ltd). negatively stained with 5% ammonium molybdate (Sigma), washed with H_2O (*x*2), drained and observed at 100.000 eV with JEOL (JEM-2100) TEM. For demonstration of antibody presence on MAb-LIPs and DUAL, LIPs were allowed to react "on grid" with 10 nm gold-labeled rabbit anti-mouse secondary antibody for 30 min. As mentioned above, this test is only used as proof of MAb immobilization on vesicles, and not for calculation of the exact number of MAbs present on the vesicle formulations used for *in vitro* and *in vivo* evaluations (since the incubation between the sample and the immune-nanogold is performed on grid).

Cell Uptake and Monolayer Transport Studies

Immortalized human brain capillary endothelial cells (hCMEC/D3) (passage 25–35) were used. The cell line was obtained under license from Institut national de la Sante et de la Recherche Medicale (INSERM, Paris, France). Cells were seeded at 27,000 cells/cm^2 and grown in EBM-2 medium (Lonza, Basel, Switzerland) supplemented with 10 mM HEPES, 1 ng/ml basic FGF (bFGF), 1.4 μM hydrocortisone, 5 μg/ml ascorbic acid, penicillin-streptomycin, chemically defined lipid concentrate, and 5% ultralow IgG FBS. The cells were cultured at 37°C, 5% CO_2/saturated humidity. All cultureware were coated with 0.1 mg/ml rat tail collagen type I (BD Biosciences). Medium was changed every 2–3 days.

Cell Uptake Studies

For LIP uptake by cells, FITC-dextran-labeled vesicles were incubated with confluent monolayers of hCMEC/D3 cells (200 nmoles liposomal lipid/10^6 cells) in medium (containing 5% (v/v) FCS) at 37°C, for 60 min, then washed in ice-cold PBS (×3), detached from plates, re-suspended in PBS and assayed by FI (after cell lysis in 2% Triton X-100). Cell auto fluorescence was always subtracted. Control experiments were carried out with free FITC-dextran at amounts similar with those encapsulated in the LIPs, and under identical conditions with the LIP/cell interaction studies, in order to exclude the possibility of uptake of dye which may have leaked out of some LIPs; the FI values measured were null. In a second set of experiments the uptake of the various LIP formulations by

cells was evaluated in presence of cell medium containing higher amounts of FCS (10, 20 and 50% v/v). All other conditions were kept constant.

Cell-Monolayer Permeation Studies

For transport experiments hCMEC/D3 cells were seeded on type I collagen pre-coated Transwell filters (polycarbonate 6 well, pore size 0.4 um; Millipore) at 5×10^4 cells/cm^2. Medium was changed every 4 days and transport assays were performed 12–15 days after seeding. 24 h before experiment, medium was replaced with fresh containing 1 nM simvastatin. Monolayer integrity was periodically inspected and the transendothelial electrical resistance (TEER) was monitored with Millicell ERS-2 (Millipore). Monolayer quality was tested by measuring LY permeability) as described (14,25), and comparing values calculated with previously reported ones (30,31). Transport experiments were conducted in HBSS (PBS + $MgCl_2$ and $CaCl_2$) supplemented with 10 mM HEPES and 1 mM sodium puryvate. A second set of transport experiments for some LIP formulations (PEG-LIP and APOe-LIP) were conducted in cell culture medium supplemented with different amounts of FCS (5 and 20% v/v). All other conditions were kept constant.

Transport was estimated after placing LIPs (labeled with FITC-dextran and RHO-Lipid) on the upper side of monolayers (200 nmoles lipid/well) and measuring FI of FITC and RHO at 15, 30 and 60 min. In all cases LY permeability was also calculated, to ensure that the vesicles did not disrupt the barrier and enhance paracellular transport. Control experiments using free FITC-dextran at the same concentrations with those entrapped in the LIP samples were also carried out (under identical conditions with the LIP permeability studies), and it was proven that at the specific conditions no FITC-dextran was transported.

Cytotoxicity Assay

The cytotoxicity of all LIP formulations used, towards hCMEC/D3 cells, was evaluated as previously reported (25). See Supplementary Material for details.

Biofluorescence Imaging

FVB mice, purchased from Hellenic Pasteur Institute (Athens, Greece) were bred at the Center for Animal Models of Disease, University of Patras, Faculty of Medicine (Rio, Greece). FVB mice were used, chosen for their white skin and fur that permits enhanced light penetration. Animal care and experimental procedures were approved by the Veterinary Administration Bureau of the Prefecture of Achaia, Greece, and were conducted according to European Union Directive 86/609/EEC for animal experiments (http://ec.europa.eu/environment/chemicals/lab_animals/legislation_en.htm). Mice used for experiments were sex-, weight (20–25 g)-, and age (6–12 weeks)-matched. Biofluorescence imaging of living mice and explanted murine organs was done on an IVIS Lumina II imager (Perkin Elmer, Santa Clara, CA). For this, mice were anesthetized using isoflurane and serially imaged at various time-points post-fluorophore-labeled NC injection, using three different excitation/emission wavelengths to detect FITC (excitation: 445–490 nm; emission: 515–575 nm), rhodamine (excitation: 500–550 nm; emission: 575–650 nm), and DiR (excitation: 710–760 nm; emission: 810–875 nm). Images were acquired and analyzed using Living Image v4.2 software (Perkin Elmer, Santa Clara, CA). In detail, bodily area- or explanted organ-specific regions of interest were created and were superimposed over all images acquired in a uniform fashion. Subsequently, photon flux within these regions was measured and compared between mice receiving different treatments.

To determine if the brain-targeted LIPs are preferentially distributed to the brain after intravenous injection, DiR was selected as ideal fluorophore for LIP labeling (15). DiR-labeled LIPs were engineered, by incorporating the dye [0.2 mol% (of total lipid)] in their lipid membrane (during their preparation). FVB mice were randomly allocated to treatment with one of each LIP type, *via* tail vein injection, ($n = 6$ mice/group). Two doses, 4 mg lipid/mouse [high dose] and 50 ug lipid/mouse [low dose], and two different ligand densities (0.1 mol% and 0.2 mol%) were used, in order to investigate their effect on the *in vivo* results. Free DiR is rapidly eliminated from mice following tail vein injection (15), as verified in the current setting by injecting 2 animals.

Statistical Analysis

All results are expressed as mean±SD from at least three independent experiments. The significance of variability between results from various groups was determined by two-way-ANOVA (for significance of interaction, time and ligand) followed by Bonferroni tests for individual differences between groups.

RESULTS

LIP Structure and Physicochemical Characteristics

As mentioned above, in addition to the MAb against the transferrin receptor, a peptide derivative of APOe3 was also used as a second brain-targeting ligand. In fact, two forms of aminoacid residues 141–150 of human APOe peptide, the monomer, and its tandem dimer repeat (141–150) were synthesized (see Materials and Methods section for details) and after immobilization on LIPs they were compared for their

targeting potential. The sequence CWG-(LRKLRKRLLR)-NH2 (M = 1698.18 g/mol), corresponding to AA residues 141–150, is referred as ApoE monomer, and the sequence CWG-(LRKLRKRLLR)-(LRKLRKRLLR)-NH2 (M = 3030.94 g/mol), corresponding to tandem sequence (141–150) is referred as APOe dimer.

The theoretical structure of APOe, MAb and DUAL-LIPs is shown in Fig. 1a–c. All types of LIPs were visualized by negative stain TEM. Colloidal-gold-immunoparticles (CGIP, with diameter of 10 nm) were used to verify MAb attachment on MAb-LIPs (Fig. 1e) and DUAL-LIPs (Fig. 1f); no MAbs where visualized on the surface of APOe-LIPs, as expected (Fig. 1d). It must be understood that CGIP binding is a qualitative test, used only for verification of the presence of MAb on the vesicle surface, and not quantitative (for exact measurement of MAb attachment yield), since the interaction between LIPs and gold-immunoparticles is carried out only for 30 min, and furthermore 'on-the-grid' where the system is constrained (and not mixed) and consequently not as "free" to interact as a simple dispersion in a test tube. Additionally, as a consequence of the fact that vesicles are dehydrated for TEM observation, the vesicle sizes observed in TEM micrographs may not be in very good agreement as those measured by DLS. The mean diameters of all LIP-types used for *in vitro* and *in vivo* evaluation, are below 160 nm (Table I). Vesicle mean diameters increase by 9–17% when DiR is incorporated in their lipid membrane (for imaging studies), as anticipated due to the fact that this lipophilic dye is incorporated in the lipid-bilayer of the vesicles. Also, the DUAL-LIPs are slightly larger than MONO-LIPs, and control PEG-LIPs, as an expected effect of the presence of two ligands on their surface. Another factor which has a slight impact on LIP size is the density of the ligands on the LIP surface (Table I). In all cases, the polydispersity index (PI) of formulations was low (< 0.25), indicating that dispersions have narrow size distribution (Table I). Furthermore, the size of all the LIP types constructed was found to be stable after (at least) a 10 day incubation period at 4°C (for most of the samples the study was continued up to a month), verifying their physical stability. In the cases of APOe decorated LIPs, decoration with monomer or dimer forms of the peptide had no effect on the vesicle size distribution or polydispersity index.

For verification that APOe peptide attachment on the surface of LIP is due to a specific interaction between the MAL groups (not verified previously (27,28)), control experiments were carried out (under identical conditions) with non-MAL liposomes. It was demonstrated that when the PEG-coating of LIPs was 2.6 mol% (of total lipid) all the amount of peptide attached on the LIPs was due to non-specific interactions, most possibly due to the 'mushroom' conformation of the PEG chain in which the MAL-groups are 'hidden' and thus not available to interact with the thiol groups of the peptide. After optimizing the LIP lipid composition (to attain the so called 'brush' conformation for surface PEG chains), the attachment yield of APOe (monomer or dimer) on LIPs was always close to 100% (Supplementary Material).

As seen in Fig. 2a, calcein-entrapping LIPs are stable and retain their content during 24 h of incubation in buffer. In presence of FCS (80% v/v), a slight release of calcein (22% of initially entrapped amount) was observed only from DUAL-LIPs after 24 h of incubation. When the retention of FITC-dextran (MW 4000), a larger molecule (compared to calcein)

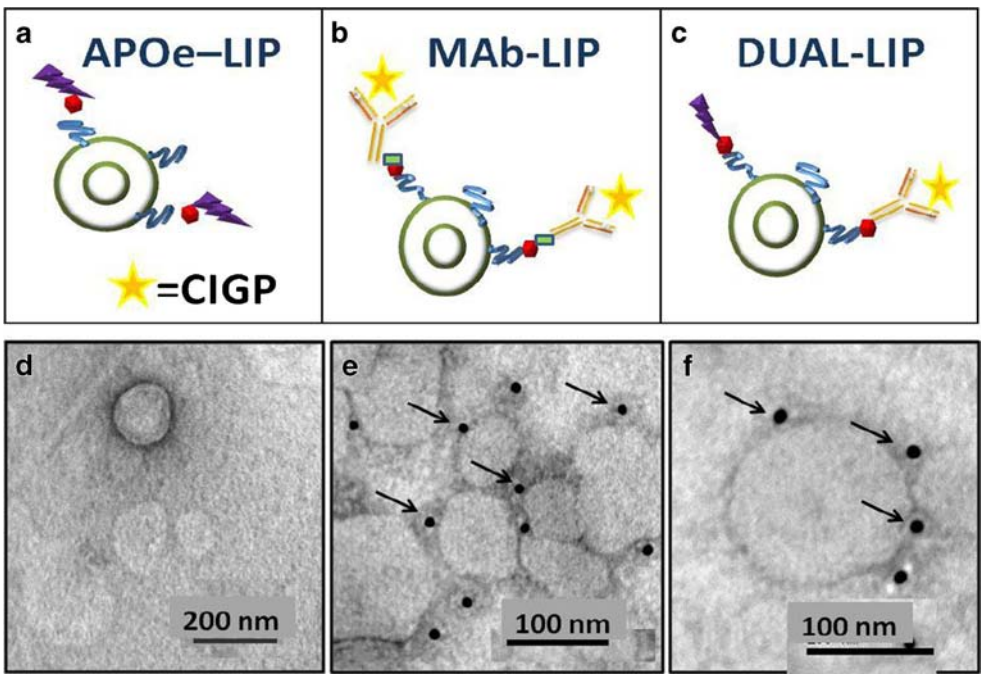

Fig. 1 (**a**–**c**) Theoretical structure of APOe-LIPs, MAb-LIPs and DUAL-LIPs; TEM images of: (**d**) APOe-LIP (**e**) MAb-LIPs and (**f**) DUAL-LIP, all after reaction with colloidal-gold-immune-particles [CGIPs]. *Arrows* point at CGIPs.

Table I LIP Mean Diameter, Polydispersity Index (PI) and ζ-Potential of all LIP Types Constructed. All Values are Means (and Corresponding SDs), from Three Different Preparations. Significant Differences Between Decorated LIP Types and Corresponding Control LIPs (PEG-LIPs with Same Label) are Indicated by *$p < 0.05$ and **$p < 0.01$

NL type	Mean Diameter (nm)	PI	Z-Potential (mV)
PEG-LIP$^{(Calcein/DiR)a}$	90.1 ± 1.4/103.9 ± 2.9	0.16/0.21	−2.38 ± 0.33[e]
APOe-LIP$^{(Calcein/DiR)a}$	128 ± 26/136.2 ± 3.6**	0.20/.022	−4.25 ± 0.59 [e]
MAb-LIP$^{(Calcein/DiR)a}$	125.0 ± 8.8 */129.7 ± 4.1**	0.19/0.18	−3.44 ± 0.54 [e]
DUAL$_{(OX\ 26)}$ $^{(Calcein/DiR)a}$	133 ± 14 */141.1 ± 3.4**	0.16/0.23	−3.3 ± 1.3 [e]
PEG-LIP $^{(Calcein/DiR)b}$	117.9 ± 2.3/120.8 ± 4.5[d]	0.17/0.18	−6.4 ± 1.6 [f]
APOe-LIP $^{(Calcein/DIR)b}$	136.2 ± 3.5 **/152.6 ± 1.7 [d]**	0.19/0.11	−7.0 ± 2.7 [f]
MAb-LIP$^{(Calcein/DiR)b}$	126.2 ± 4.1**/144.4 ± 3.4 [d]**	0.18/0.16	−4.61 ± 0.61 [f]
DUAL$_{(RI7217)}$ $^{(Calcein/DIR)b}$	139 ± 11*/158.4 ± 3.0 [d]**	0.19/0.23	−7.3 ± 2.3 [f]/-4.40 ± 0.37 [e]
DUAL$_{(OX26)}$ $^{(FITC)c}$	143.8 ± 8.1 [d]	0.25	−3.95 ± 0.47 [e]

[a] Liposome types used in *in vitro* studies [low density of ligands 0.05 mol%]

[b] Liposome types used *in vitro*/*in vivo* studies [double density of ligands 0.1 mol%]

[c] Liposomes with triple ligand density (0.15 mol%) used for *in vitro* studies

[d] <6% increase of mean diameter after 1 week at 4°C

[e] Calcein or FITC-encapsulating liposomes

[f] DiR-incorporating liposomes

was followed, it was demonstrated to leak from DUAL-LIPs at a lower rate (compared to calcein) (Fig. 2b), and the DUAL-LIP integrity was similar to that of control PEG-LIPs and not affected by the presence of the two ligands on the vesicle surface. All other LIP types constructed had similar FITC retention values, and are not shown in the graph for clarity. When the FITC-dextran encapsulating LIPs were incubated in cell culture medium, FITC-dextran was totally retained in all LIPs studied for at least up to 3 h or co-incubation (not shown), confirming that the uptake of this dye (calculated by the FI of disrupted cells after they have been incubated with LIPs and thoroughly washed) is a reliable value to use for the calculation of the uptake of LIPs by cells (since the FITC-dextran/lipid ratio remains stable under the conditions applying during cell/LIP incubation), as reported also previously (14,25). DUAL and MONO LIPs with double amount of ligands on their surface [0.2 mol%] (Fig. 2c), were found to be considerably more "leaky" compared to the corresponding formulations with half the amount of ligands on their surface [0.1 mol%], when incubated in FCS (Fig. 2a). When ligand density on DUAL LIPs was further increased to 0.3 mol%, their integrity in FCS was reduced even more (compared to 0.2 mol% ligand density) [not shown for clarity]. DUAL- LIPs with ligand density of 0.2 mol%, retain their calcein-content during 5 h of incubation in serum proteins and then gradually loose between 40% and 60% during the following 19 h of incubation. However, (since again a small hydrophilic dye (calcein) was used), it is anticipated that larger and more hydrophobic agents will be retained for longer periods. It is important to state at this point that the observed leakage of calcein does not, in any way, affect the reliability of the *in vivo* results, since the lipophilic dye DiR (which is incorporated in the lipid membrane and not encapsulated in the aqueous interior of the vesicles), was the liposome-associated-label followed in those studies.

Cell Toxicity

After verifying the techniques selected for preparation of the various types of MONO and DUAL LIPS and investigation of the brain targeting capabilities, it was essential to be sure that all types of LIPs are not toxic against the cellular model selected for *in vitro* studies. For this, LIPs were tested for cytotoxicity towards hCMEC/D3 cells (by the MTT assay), after 24 h of incubation with the cells (similar concentrations with those planned to be used in the LIP/cell interaction studies). Results indicate that all liposomes used are non-toxic for these cells (Supplementary Material).

LIP-Cell Interactions

LIP uptake by hCMEC/D3 cells was studied as a first *in vitro* test to explore their BBB targeting potential. It was recently verified that the interaction between hCMEC/D3 cells and OX-26-decorated-LIPs is rapid, and that their uptake by cells reaches a high value after only 15 min of incubation; while the uptake value is constant for 1 and 2 h of incubation (14). On the other hand, the non-targeted LIP-type uptake increases with time, since the non-specific mechanisms by which they are taken up (by cells), are of lower velocity. Thereby, in order to compare the targeting potential of the different types of targeted and control LIPs, a 1 h incubation period was used.

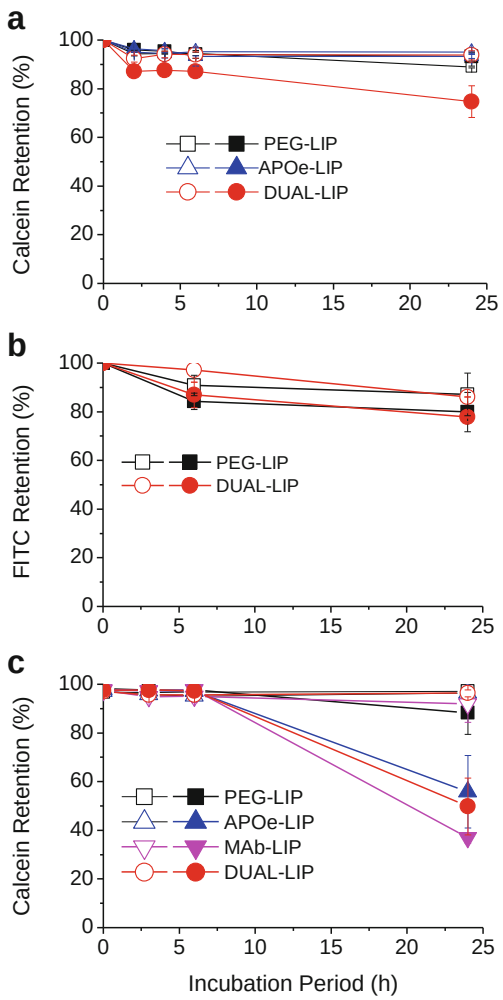

Fig. 2 (**a**) Retention of calcein in LIPs during incubation in buffer (*hollow symbols*) or 80% v/v Fetal Calf Serum (FCS) (*solid symbols*), for 24 h at 37°C. The density of ligands on the surface of the vesicles was 0.1 mol% of total lipids (**b**) Corresponding results for the retention of FITC-dextran (4000) in the same LIP formulations studied above, under identical incubation conditions. (**c**) Retention of calcein in LIPs with double density of ligands on their surface compared to those in graph A [0.2 mol% of total lipids], during incubation in buffer (*solid symbols*) or 80% v/v Fetal Calf Serum (FCS) (*hollow symbols*), for 24 h at 37°C. Each value is the mean of 4 samples, and *bars* represent SDs of each mean. Symbol keys are in graph inserts.

Cell uptake results show that the uptake of all LIPs with surface attached ligands, is significantly higher compared to LIPs with no ligand on their surface (PEG-LIP) (Fig. 3), and MAb-LIP uptake (1.86 ± 0.30 nmoles of lipid per 10^6 cells) is similar to the previously reported value (14). In addition, APOe-LIP uptake is significantly higher (2.3–2.5 times) compared with PEG-LIPs, in agreement with recently published results (27,28), although a much lower ligand density was used in the current study. No significant difference was observed between the uptake values of LIPs decorated with monomer or dimer APOe peptide ($p > 0.05$). Due to the toxicity observed following *in vivo* administration of dimer-decorated APOe LIPs, which was not seen when the monomer peptide was used, all the following studies were performed using the

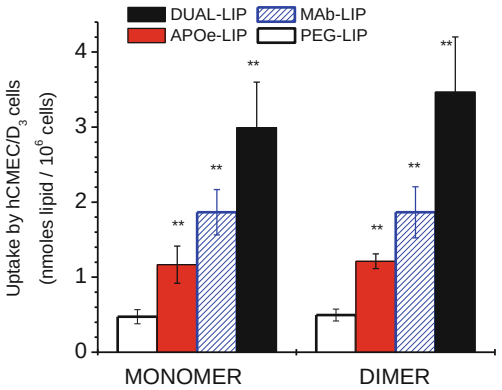

Fig. 3 Uptake of MONO and DUAL LIP types by hCMEC/D3 cells. Uptake is expressed as nmoles lipid taken up by the cells (calculated from FITC dextran FI). The monomer and dimer forms of APOe peptide were used for LIP decoration (where appropriate). Each value is the mean of at least 3 experiments and bars are SDs of means. *Asterisks'* correspond to significant differences between control vesicles (PEG-LIP) and specific LIP-type.

monomer APOe, despite the more physiological nature of the dimer form.

The cell-uptake of DUAL-LIPs was further increased compared with both MONO-LIP formulations, while their uptake (3.0–3.5 nmoles of lipid per 10^6 cells) practically equaled the additive uptake values for the two types of MONO-LIPs (APOe-LIP+MAb-LIP). This confirmed that at the specific ligand density used, which corresponds to approx. 10 (MAb) + 14 (APOe) ligand molecules on the vesicle surface (calculated for vesicles with mean diameter ~ 150 nm, and taking into account the mean attachment yields calculated for each ligand, for the number of vesicles present in a dispersion with specific concentration (which was estimated from a previously published nomogram [relating theoretical captured volume, diameter, number, area, and lipid weight of unilamellar liposomes]) (24), there is no interference between the two ligands; an important observation, since it was previously demonstrated (*in vitro*) that the addition of a second non-specific IgG antibody (in same amount) on (OX-26) MAb-LIPs results in a 15% decrease of their uptake by hCDMEC/D3 cells (14). Thereby, perhaps the use of peptide/antibody combinations may be a solution for overcoming such interferences in dual targeted nanoparticle systems.

The effect of ligand surface density of DUAL-LIPs on their interaction with hCMEC/D3 cells was also evaluated and found to increase LIP uptake (by hCMEC/D3 cells) in a linear way (Fig. 4), when increased from 0.1 to 0.3 mol% (of total lipid). However, as the ligand density on LIPs increases from 0.1 to 0.3 mol%, their integrity when incubated in serum proteins is significantly decreased compared to the targeted LIP types with lower ligand density (as mentioned above), possibly due to increased interactions between adjacent ligand molecules (since they are closer to one another), as seen in the results of the LIP integrity studies (Fig. 2). For this reason when selecting appropriate ligand densities for development of

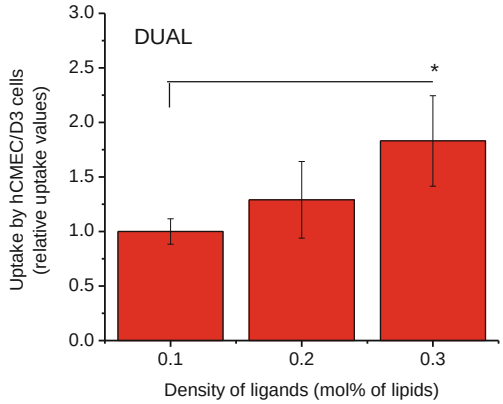

Fig. 4 Effect of surface-ligand density (cumulative value for both ligands used) on the uptake of DUAL- LIPs by hCMEC/D3 cells. The two ligands were used at equimolar amounts. The uptake is expressed as relative uptake compared with the formulation with lowest ligand density (0.1 mol% [compared to total lipids]). Each value is the mean of at least 3 experiments and bars are SDs of means.

targeted LIPs, both of these factors should be considered. Herein, the 0.1 mol% and 0.2 mol% ligand densities were used in the *in vivo* studies.

LIP Transport Studies

LIP transport experiments were performed using HBSS in the donor phase of the transwell-cultured monolayers. TEER of the monolayer was 59.8±6.3 Ω cm^2 (after simvastatin treatment) and lucifer yellow (LY) permeability ranged between $1.1\times10^{-3}-1.432\times10^{-3}$ cm/min, in good agreement with previously reported values (30). LY permeability was also measured in each specific monolayer used for LIP-BBB transport evaluations, and no significant differences were detected in any case, proving that the monolayer permeability was not affected by any LIP-type evaluated. As seen in Fig. 5, for all LIPs there is a gradual increase in transport of both liposome-associated labels, FITC-dextran (Fig. 5a) and RHO-lipid (Fig. 5b), with time. Permeability values are 5.03×10^{-5} ($\pm$ 0.91×10^{-5}) cm/min for the PEG-LIP, 9.25×10^{-5} ($\pm$ 1.42×10^{-5}) cm/min (equal) for both APOe-LIP and MAb-LIP, and 20.5×10^{-5} ($\pm$ 3.8×10^{-5}) cm/min for DUAL-LIP.

After 60 min incubation DUAL-LIP transport is significantly higher compared to all other LIPs evaluated. In fact, transport of DUAL-LIPs is almost equal to the added values (% transport) of the two MONO-LIPs (4.01 *versus* 2.00+1.68 [for FITC transport] or 4.00 *versus* 2.41+2.38 [for RHO transport]). The results also confirm that all LIP types are transported through the monolayer in intact form, since transported amounts of the two markers are similar. Indeed, FITC/RHO ratios are close to 1.00 in all cases (Table II).

In Vivo and *Ex Vivo* Studies

Imaging results (Fig. 6a) show that at 4 h post-injection, brain-targeted DUAL-LIPs achieved close to 40% higher head

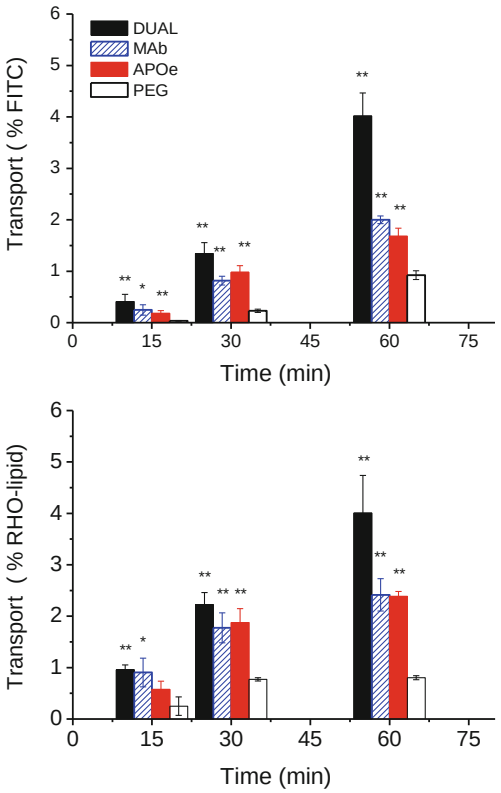

Fig. 5 Transcytosis of LIPs through hCMEC/D3 monolayers. LIPs were added on transwell-mounted monolayers and transport was calculated by FITC FI (upper graph) and RHO-lipid FI (lower graph) at 15, 30 and 60 min. Each value is the mean of at least 3 experiments. *Asterisks* denote significant differences between specific LIP-types and PEG-LIP.

fluorescence emission levels compared with PEG-LIP (controls), while the APOe-LIP-receiving mice head fluorescence was only slightly (~20%) but not significantly increased (compared to PEG-LIPs), for the high-dose/low-ligand density *in vivo* study. The later result was verified by imaging the explanted brains immediately post-mortem (Fig. 6b) (*ex-vivo* measurements), confirming a 53.5% increased brain delivery of DUAL-LIPs ($p<0.01$) and slight - non-significant- increase for APOe-LIPs. When the low-lipid dose was used (in case the high dose blocked identification of biodistribution differences, due to organ saturation), and the surface ligand-density on LIPs was doubled (in case the density used initially was not

Table II Average Values of Ratios (Mean Values Calculated from Individual Ratio Values) of Transported LIP-Associated FITC-Dextran/RHO-Lipid, after 60 min Incubations of the Corresponding LIPs with hCMEC/D3 Monolayers. Reported Values are the Mean Values Calculated from at Least four Independent Experiments (± SD's of Means)

NL-type	FITC/RHO (% transport) ratio 60 min
PEG-LIP	1.19±0.16
ApoE-LIP	0.95±0.31
MAb-LIP	0.88±0.18
DUAL-LIP	1.05±0.21

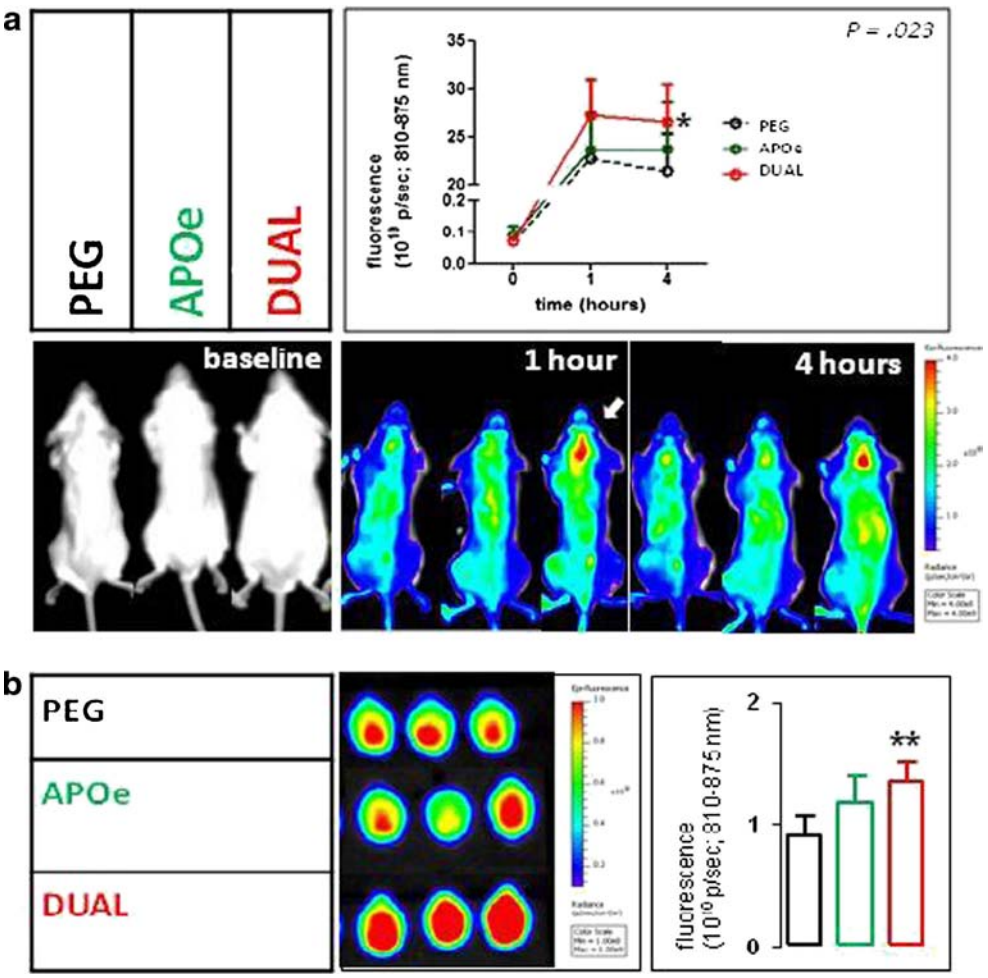

Fig. 6 Results of first *in vivo* study: (**a**) Representative biofluorescence images of animals receiving 4 mg of PEG-LIP; APOe-LIP and DUAL-LIP at 0 h (pre-administration) 1 and 4 h post-administration (brain-targeting indicated by arrows). Mean fluorescence (photons/s) values at each time point (from 6 animals per group) are shown in the inserted graph. (**b**) Representative images of explanted brains (immediately post-mortem). The corresponding mean fluorescence values (photons/s) ($n = 6$) are shown in the inserted bar graph.

sufficient for *in vivo* targeting), both, the live imaging results (Fig. 7, upper panel) and the *ex vivo* imaging results (Fig. 7, lower panel) show that at 24 h post-injection brain distribution of DUAL-LIP is 2.1–2.6 times higher compared to PEG-LIPs ($P < 0.0001$) and also significantly higher than APOe-LIP. In both sets of data from this second *in vivo* study, *in vivo* and *ex-vivo* (brain values and also brain/liver ratios), the effect of the ligand was calculated as highly significant by one-way ANOVA analysis, verifying that indeed brain targeting was proven. The targeting capability of MAb-LIPs is also significantly higher compared to PEG-LIPs, which is not the case for APOe-LIPs which have similar brain levels with the PEG-LIPs up to 16 h post injection and only slightly higher after 24 h, however the difference is not significant (as also in the *ex-vivo* values).

The *in vivo* results for the APOe-LIPs from both *in vivo* studies, do not agree with the data derived from *in vitro* tests, in which it was observed that these LIPs can target the brain substantially better than PEG-LIPs.

During the two *in vivo* studies carried out, no *in vivo* toxicity of the MONO or DUAL-LIPs was noticed, even when high dose of LIPs was used, providing that the liposome mean diameter was below 200 nm. In some cases, when larger size LIP batches were injected at high dose (4 mg lipid per mouse) toxicity was observed, which was not the case when low dose was used (50 ug per mouse).

In Vitro Studies in Presence of Serum Proteins

In the light of recent findings about the importance of interactions between ligand-targeted nanosystems and serum components (29), additional *in vitro* cell uptake and cell-monolayer transport studies in presence of increasing amounts of serum (10, 20 or 50% v/v concentrations of FCS in cell culture medium, for uptake studies, and 5 or 20% v/v concentrations of FCS in cell culture medium, for the transport studies), were carried out in order to gain insight about the different *in vivo* behavior (capability to target the brain) of APOe-LIPs and MAb-LIPs, and the contradictory *in vitro*/*in vivo* results. As seen in Fig. 8, very interestingly, as the protein content of the medium increases the cell uptake of some LIP types are affected more than others. More specifically, when increasing FCS from 10 to 50%, the cell uptake of APOe-LIP decreases to approx. 30% of the initial value, while at the same time the uptake of PEG-LIPs is practically doubled. Oppositely, the

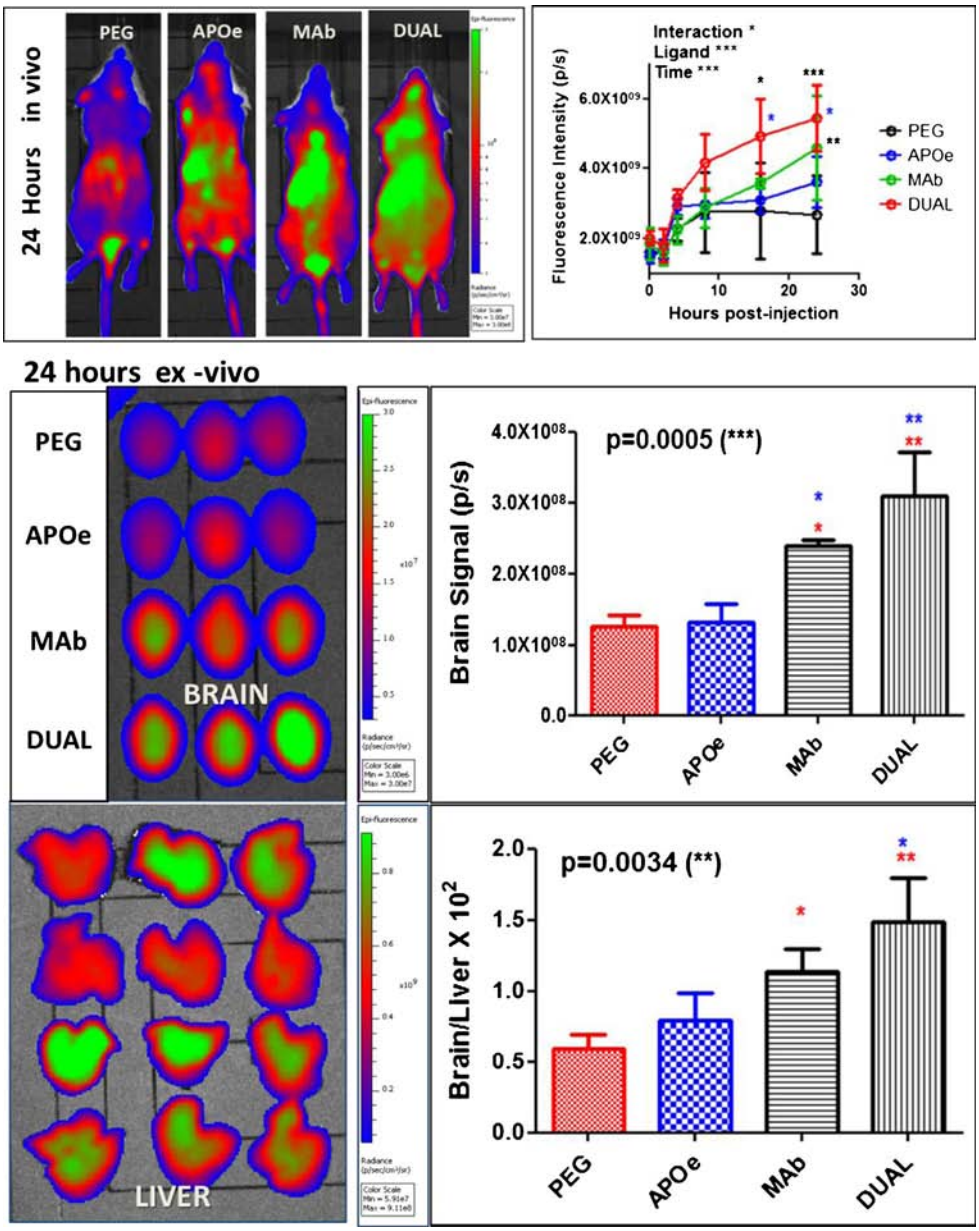

Fig. 7 Results of second *in vivo* study. *Upper panel* Representative biofluorescence images of animals receiving 50 μg of PEG-LIP; APOe-LIP, MAb-LIP and DUAL-LIP at 0 h (pre-administration) 2, 4, 8, 16 and 24 h post-administration. Mean fluorescence (photons/s) values at each time point (from 3 animals per group) are shown in the inserted graph. *Lower Panel* Representative images of explanted brains and livers (immediately post-mortem). The corresponding mean fluorescence values (photons/s) are shown in the inserted bar graphs.

interaction of MAb-LIPs is not significantly affected by the presence of serum proteins, at this FCS concentration range (10–50%), however the DUAL-LIPs uptake is considerably (~35%) reduced when FCS concentration is increased from 5 to 50%, most possibly due to the "inactivation" of the APOe-peptide ligand, which contributes now less (or not at all) in the overall degree of uptake. Furthermore, the presence of increased serum protein concentrations results in decreased interaction with hCMEC/D3 cells also when the ligand surface density of DUAL-LIPs is doubled (lower graph in Fig. 8). In any case, at FCS concentrations which are higher than 20% (v/v) there is no significant difference (in terms of uptake by hCMEC/D3 cells) between MAb-LIPs and DUAL-LIPs. The later result implies that in presence of serum proteins, MAb-LIPs with double ligand density will perform better than DUAL-LIPs to target the brain, due do the effect of serum proteins on APOe-LIPs.

Similar effects of serum proteins on the targetability of APOe-LIPs were also observed, when it was assessed by monolayer transport. Indeed, as seen in Fig. 9, the transport of APOe-LIPs across hCMEC/D3 monolayers is significantly decreased when the study is performed in presence of 5% or 20% serum proteins, while under identical conditions PEG-LIP transport is significantly increased (Fig. 9a). Since the permeability of the monolayers was slightly influenced by the proteins (Fig. 9b), APOe-LIP transport was also expressed as relevant value (by comparing with PEG-LIP transport under identical experimental conditions). As seen (Fig. 9c),

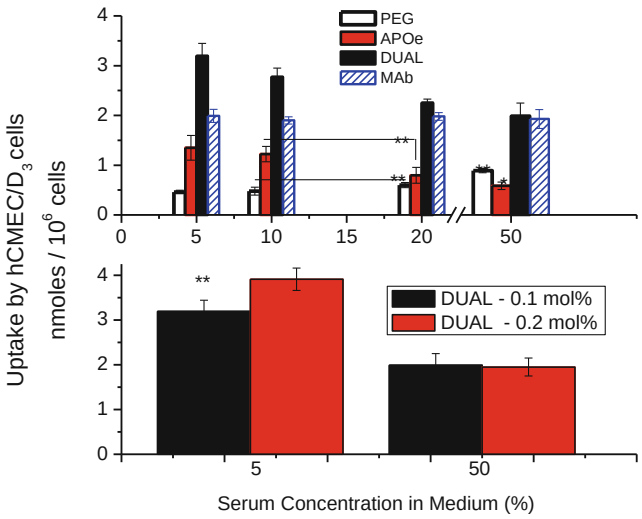

Fig. 8 Effect of serum concentration (mixed in the cell medium) on the uptake of LIPs by hCMEC/D3 cells. Uptake is expressed as nmoles lipid in cells (calculated from FITC dextran). Each value is the mean of at least 3 experiments and bars are SDs of means. The *upper graph* is for LIPs decorated with 0.1 mol% (compared to total lipid) ligands, while the lower graph also shows results obtained with double density (0.2 mol%) DUAL-LIPs.

although the transport of APOe-LIPs was more than two times higher compared to PEG-LIPs when studies were carried out in HBSS, the value was drastically decreased when the experiment was carried out even in 5% serum, approaching the value of PEG-LIP transport (relevant value was close to 1). When the serum concentration was increased to 20%, APOe-LIP relevant transport value became lower than 1. Furthermore, similar results in presence of serum were observed even when the APOe-peptide density on the LIP surface was doubled, although transport was increased by 17%, when studied in HBSS.

DISCUSSION

Targeted nanoparticulate systems can be decorated with different targeting ligands, to increase their delivery to extracellular or intracellular compartments. This strategy has been investigated with good results by constructing LIPs coupled to antibodies targeting TfR and human insulin receptor (36) or TfR and E-selectin (37). Recently, dual-targeting daunorubicin LIPs with mannose and transferrin (Tf) were demonstrated to target higher quantities of drug to brain glioma (17), while doxorubicin-loaded HSA nanoparticles with two ligands were found to be superior to target cancer cells compared to one ligand systems (20). Additionally dual-ligand LIPs with RGD and cell penetrating peptides were characterized as effective tools to accelerate cellular uptake (19), while aptamer plus peptide dual-decorated nanoparticles (NPs) were found to target brain glioma better compared to one-ligand-NPs (21).

Herein, we investigated whether the previously (*in vitro*) demonstrated brain-targeting potential of anti-TfR MAb-decorated LIPs, can be further enhanced by addition of a second ligand, which has been recently proven (*in vitro*) to target brain cells (27,28), and furthermore whether an established BBB cellular model can be used for prediction of *in vivo* performance of such targeted formulations. A peptide

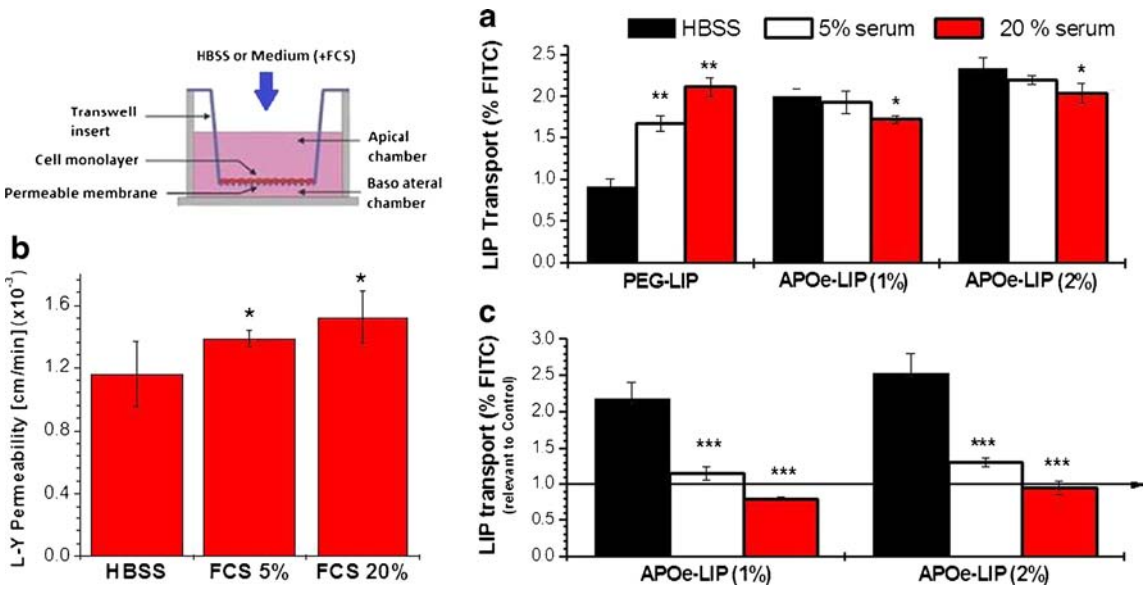

Fig. 9 Effect of serum concentration (mixed in the cell medium) on the transport of APOe-LIPs across hCMEC/D3 monolayers. Uptake is expressed as% liposome-associated-FITC transported (calculated from FITC FI). Each value is the mean of at least 3 experiments and bars are SDs of means. *Right-side graphs* Upper graph shows absolute transport values for APOe-LIPs decorated with 0.1 and 0.2 mol% (compared to total lipid) peptide-ligands, and corresponding values for PEG-LIPs, while the lower graph shows relevant transport values (as compared to PEG-LIPs). The effect of serum concentration on L-Y permeability is presented in the left-side graph.

derivative of APO-E_3, was constructed in its dimer and monomeric form, and after optimizing preparative conditions for successful attachment of the peptide on LIPs, DUAL- LIPs were constructed. After confirming that LIP characteristics (size distribution, *etc.*) are sufficient for *in vivo* use (Table I and Fig. 2), the DUAL-LIPs (as well corresponding MONO-LIPs) were screened *in vitro* for their cytotoxicity and for uptake by brain cells and transport across a BBB cellular model (Figs. 3 and 5). In all *in vitro* experiments, results demonstrated significantly improved brain targeting capability (higher uptake by cells and permeability across BBB cell-model monolayer) of the DUAL-LIPs compared to the formulations with no ligands (plain PEG-LIP) or MONO-LIPs (one ligand), while MONO-LIPs also performed significantly better than PEG-LIPs (in good correlation with the results of recent studies) (27,28). Additionally, no cytotoxicity was observed. The increased uptake/transport of APOe-LIPs across hCMEC/D3 monolayers, is explained since these cells over-express low-density lipoprotein receptor related protein (LPR) (relevant data presented in Supplementary Material), while the performance of the MAb-LIPs is due to the tranferrin receptor on hCMEC/D3 cells, as proven recently (14).

Two *in vivo* live-animal imaging studies, using DiR (15,38) confirmed the brain targeting capability of DUAL-LIPs (Figs. 6 and 7), despite the fact that the ligand density used is from 1.5 to 5 times lower compared to other dual ligand nanoparticles (17,19–21). However, the differences (in terms of brain-targeting capability) between the various LIPs-types evaluated *in vivo*, could not be predicted by the *in vitro* uptake or monolayer permeability studies, especially since the control PEG-LIPs were seen to give similar *in vivo* (and *ex vivo*) brain levels with those attained by APOe-LIPs, while the presence of APOe-petide ligand on DUAL-LIPs, did not significantly increase the targeting capability of MAb-LIPs. The comparably high brain levels of PEG-LIPs may be attributed to surface-adsorption of systemically available proteins, known to enhance brain transport of polymer-coated nanocarriers (39–41). Furthermore, despite the fact that optimal ligand surface densities and ligation techniques may need to be identified in order to obtain the highest targeting capability for each specific formulation (42–45), the disagreement between *in vitro* and *in vivo* results for the LIP-types evaluated here in, cannot be attributed to any such potential shortcomings. In the light of recent finding about the importance of interactions between ligand-targeted nanosystems and serum components, we performed additional *in vitro* cell-LIP interaction studies in presence of increasing amounts of serum, in order to investigate if perhaps such *in vitro* test can provide better explanation of what may be taking place *in vivo*. Very interestingly, the results of the modified *in vitro* uptake studies (Fig. 8) were better correlated with the *in vivo* results (compared to the *in vitro* studies carried out initially (Figs. 3, 4, and 5) for both MONO- and DUAL-LIP types, suggesting that such modified *in vitro* tests could provide useful insights for *in vivo* performance of such targeted nanosystems (with one or two ligands), in accordance with recent suggestions (29).

Nevertheless, the *in vivo* uptake of LIPs by the brain is a complex phenomenon which is most possibly affected by several procedures between which the kinetics of the vesicles in the circulation, their bio-distribution (which will affect the time it takes for the vesicles to reach the brain endothelial cells, and the percent of them that do this), their stability in the blood and their targeting potential (in the form that they are when they reach the brain cells). Thereby it is difficult to have a single *in vitro* screening test that will be able to provide accurate predictions of the *in-vivo* performance of targeted-formulations. Providing that selected formulations have been screened for their integrity in presence of biological media, perhaps the monolayer transport experiment has closer resemblance to the *in vivo* case, where, the nanoformulation should translocate across the BBB to be distributed in the brain. Thereby, additional modified cell monolayer transport experiments were also carried out, in presence of serum proteins, and it was observed that APOe-LIP relevant transport (compared to that of PEG-LIPs) is substantially affected (decreased), even when only 5% of serum was used (Fig. 9), in good agreement with the modified cell uptake study (Fig. 8) and the *in vivo* study, results.

In any case, the mechanisms involved in the serum-induced modulation of LIP targetability are not clarified, and further experiments are surely required in order to elucidate why the MAb-LIPs are affected less by the serum proteins compared to the APOe-LIPs. One may postulate that perhaps the effect of serum proteins on APOe-LIP brain targeting may be due to down regulation of the low-density lipoprotein receptor related protein (LPR); However, since it is a rather fast effect (uptake after only 1 h of incubation is measured) it is highly unlikely that any cell differentiation may take place so fast (usually such events happen after at least 24 h and are initiated after about 6 h) (46). Thereby, we postulate that the most likely mechanism is the adsorption of proteins on the vesicle surface, which, most possibly, block the ability of the APOe peptide to reach (and interact with) the LPR receptor on the cell surface. This theory is perhaps more plausible, since it is known that protein adsorption on nanoparticulates injected in the bloodstream happens very fast. In fact, 5–10 min incubation periods have been used to study such events by 2D page techniques (47). On the other hand, the fact that the MAb targeting ability is not modulated at the same degree, may suggest that due to its profoundly larger size (compared to the peptide) the MAb is not blocked at the same degree as the peptide.

In any case, the results of the current experiments, suggest that modified *in vitro* (uptake or monolayer transport) studies, carried out in presence of serum proteins may be useful as predictive tools for the *in vivo* performance of targeted nanofurmulations.

CONCLUSIONS

MONO and DUAL-targeted LIPs, using two ligands to target the brain (a MAb against the transferrin receptor and an ApoE3-peptide derivative targeting the LPR [APOe]) were tested *in vitro* (on hCMEC/D3 BBB cellular model) and *in vivo* for their brain targeting capability. Oppositely to *in vitro* tests, *in vivo* results show that APOe-ligand decorated LIPs do not have increased targeting capability (compared with non-targeted LIPs) and that addition of APOe as a second ligand on MAb-LIPs does not significantly improve LIP brain-targeting capability. Interestingly, *in vitro* experiments carried out in the presence of increasing concentrations of serum proteins added in cell culture medium (5–50% v/v); prove that the targeting capability of peptide-decorated LIPs is profoundly affected by serum proteins. Such modified *in vitro* tests may be useful for *in vitro* screening of targeted nanomedicines, and may provide possible explanations about the disagreement between *in vitro* and *in vivo* results.

ACKNOWLEDGMENTS AND DISCLOSURES

E. Markoutsa and K. Papadia equally contributed to this paper. The research leading to these results has received funding from the European Community's Seventh Framework Programme (FP7/2007–2013) under grant agreements n° 212043 (to SGA) and 260524 (to GTS). Authors are grateful to Dr. Pierre-Oliver Couraud (Inserm, Paris, FR) for providing the hCMEC/D3 cell line, and Dr. M Gregori (University Milano-Biccoca, Milan, IT) for her help in MAb thiolation.

REFERENCES

1. Pardridge WM. Drug transport across the blood–brain barrier. J Cerebral Blood Flow Metabolism. 2012;32:1959–72.
2. Lu W, Xiong C, Zhang R, Shi L, Huang M, Zhang G, *et al*. Receptor-mediated transcytosis: A mechanism for active extravascular transport of nanoparticles in solid tumors. J Control Release. 2012;161:959–66.
3. Paliwal SR, Paliwa R, Agrawa GP, Vyas SP. Targeted breast cancer nanotherapeutics: options and opportunities with estrogen receptors. Critl Rev in Therap Drug Carrier Syst. 2012;29:421–46.
4. Ghosh SC, Neslihan AS, Klostergaard J. CD44: A validated target for improved delivery of cancer therapeutics. Exp Opinion on Therap Targets. 2012;16:635–50.
5. Jiang X, Sha X, Xin H, Chen L, Gao X, Wang X, *et al*. Self-aggregated pegylated poly (trimethylene carbonate) nanoparticles decorated with c(RGDyK) peptide for targeted paclitaxel delivery to integrin-rich tumors. Biomaterials. 2011;32:9457–69.
6. Wang Z, Yu Y, Dai W, Cui J, Wu H, Yuan L, *et al*. A specific peptide ligand-modified lipid nanoparticle carrier for the inhibition of tumor metastasis growth. Biomaterials. 2013;34(3):756–64.
7. Gomes-Da-Silva LC, Santos AO, Bimbo LM, Moura V, Ramalho JS, Pedroso De Lima MC, *et al*. Toward a siRNA-containing nanoparticle targeted to breast cancer cells and the tumor microenvironment. Int J Pharma. 2012;434:9–19.
8. Xin H, Sha X, Jiang X, Chen L, Law K, Gu J, *et al*. The brain targeting mechanism of Angiopep-conjugated poly(ethylene glycol)-co-poly(e{open}-caprolactone) nanoparticles. Biomaterials. 2012;33(5):1673–81.
9. Pardridge WM. Drug targeting to the brain. Pharm Res. 2007;24:1733–44.
10. Lalani J, Raichandani Y, Mathur R, Lalan M, Chutani K, Mishra AK, *et al*. Comparative receptor based brain delivery of tramadol-loaded poly(lactic-co-glycolic acid) nanoparticles. J Biomed Nanotech. 2012;8(6):918–27.
11. Xia H, Gao X, Gu G, Liu Z, Hu Q, Tu Y, *et al*. Penetration-functionalized PEG-PLA nanoparticles for brain drug delivery. Int J Pharmac. 2012;436:840–50.
12. López-Dávila V, Seifalian AM, Loizidou M. Organic nanocarriers for cancer drug delivery. Curr Opinion Pharmacol. 2012;12(4):414–9.
13. Antimisiaris SG, Kallinteri P, Fatouros D. Liposomes and drug delivery, In: S.C. Gad editor, Pharmaceutical Manufacturing Handbook Production and Processes, John Wiley & Sons, 2008, pp. 443-533.
14. Markoutsa E, Pampalakis G, Niarakis A, Romero IA, Weksler B, Couraud P-O, *et al*. Uptake and permeability studies of BBB-targeting immunoliposomes using the hCMEC/D3 cell line. Eur J Pharmaceut Biopharma. 2011;77(2):265–74.
15. Xiang Y, Liang L, Wang X, Wang J, Zhang X, Zhang Q. Chloride channel-mediated brain glioma targeting of chlorotoxin-modified doxorubicine-loaded liposomes. J Control Release. 2011;152:402–10.
16. Kluza E, Jacobs I, Hectors SJCG, Mayo KH, Griffoen AW, Strijkers GJ, *et al*. Dual-targeting of αvβ3 and galectin-1 improves the specificity of paramagnetic/fluorescent liposomes to tumor endothelium in vivo. J Control Release. 2012;158:207–14.
17. Ying X, Wen H, Lu W-L, Du J, Guo J, Tian W, *et al*. Dual-targeting daunorubicin liposomes improve the therapeutic efficacy of brain glioma in animals. J Control Release. 2010;141(2):183–92.
18. Li Y, He H, Jia X, Lu W-L, Lou J, Wei Y. A dual-targeting nanocarrier based on poly(amidoamine) dendrimers conjugated with transferrin and tamoxifen for treating brain gliomas. Biomaterials. 2012;33(15):3899–908.
19. Kibria G, Hatakeyama H, Ohga N, Hida K, Harashima H. Dual-ligand modification of PEGylated liposomes shows better selectivity and efficient gene delivery. J Control Release. 2011;153(2):141–8.
20. Bae S, Ma K, Kim TH, Lee ES, Oh KT, Park E-S, *et al*. Doxorubicin-loaded human serum albumin nanoparticles surface-modified with TNF-related apoptosis-inducing ligand and transferrin for targeting multiple tumor types. Biomaterials. 2012;33(5):1536–46.
21. Gao H, Qian J, Cao S, Yang Z, Pang Z, Pan S, *et al*. Precise glioma targeting of and penetration by aptamer and peptide dual-functioned nanoparticles. Biomaterials. 2012;33(20):5115–23.
22. Papademetriou T, Garnacho C, Schuchman EH, Muro S. In vivo performance of polymer nanocarriers dually-targeted to epitopes of the same or different receptors. Biomaterials. 2013;34:3459–66.
23. Ulbrich K, Hekmatara T, Herbert E, Kreuter J. Transferrin- and transferring-receptor-antibody-modified nanoparticles enable drug delivery across the blood-brain barrier (BBB). Eur J Pharm Biopharm. 2009;71:251–6.
24. Schnyder A, Huwyler J. Drug transport to brain with targeted Liposomes. NeuroRx. 2005;2:99–107.
25. Markoutsa E, Papadia K, Clemente C, Flores O, Antimisiaris SG. Anti-Aβ-MAb and dually decorated nanoliposomes: Effect of Aβ1-42 peptides on interaction with hCMEC/D3 cells. Eur J Pharm Biopharm. 2012;81(1):49–56.
26. Pardridge WM. Tyrosine hydroxylase replacement in experimental Parkinson's disease with transvascular gene therapy. NeuroRx. 2005;2(1):129–38.

27. Re F, Cambianica I, Zona C, Sesana S, Gregori M, Rigolio R, *et al*. Functionalization of liposomes with ApoE-derived peptides at different density affects cellular uptake and drug transport across a blood-brain barrier model. Nanomed Nanotech Biol Med. 2011;7(5):551–9.
28. Re F, Cambianica I, Sesana S, Salvati E, Cagnotto A, Salmona M, *et al*. Functionalization with ApoE-derived peptides enhances the interaction with brain capillary endothelial cells of nanoliposomes binding amyloid-beta peptide. J Biotechnol. 2010;156(4):341–6.
29. Salvati A, Pitek AS, Monopoli MP, Prapainop K, Baldelli Bombelli F, Hristov DR, *et al*. Transferrin-functionalized nanoparticles lose their targeting capabilities when a biomolecule corona adsorbs on the surface. Nature Nanotech. 2013;8:137–43.
30. Weksler BB, Subileau EA, Perriere N, Charneau P, Holloway K, Leveque M, *et al*. Blood-brain barrier-specific properties of a human adult brain endothelial cell line. FASEB J. 2005;19:1872–4.
31. Poller R, Gutman H, Krahenbuhl S, Weksler B, Romero I, Couraud PO, *et al*. The human brain endothelial cell line hCMEC/D3 as a human blood-brain barrier model for drug transport studies. J Neurochem. 2008;107:1358–68.
32. Brambilla D, Nicolas J, Le Droumaguet B, Andrieux K, Marsaud V, Couraud P-O, *et al*. Design of fluorescently tagged poly(alkyl cyanoacrylate) nanoparticles for human brain endothelial cell imaging. Chem Commun. 2010;46:2602–4.
33. Kaasgaard T, Mouritsen OG, Jørgensen K. Receptor mediated binding of avidin to polymer covered liposomes. J Liposome Res. 2001;11(1):31–42.
34. Stewart JCM. Colorimetric determination of phospholipids with ammonium ferrothiocyanate. Anal Biochem. 1980;104:10–4.
35. Kokona M, Kallinteri P, Fatouros D, Antimisiaris SG. Stability of SUV liposomes in the presence of cholate salts and pancreatic lipases: effect of lipid composition. Eur J Pharm Sciences. 2000;9:245–52.
36. Zhang Y, Zhu C, Pardridge WM. Antisence gene therapy of brain cancer with an artificial virus gene delivery system. Mol Ther. 2002;6:67–72.
37. Tan PH, Manunta M, Ardjomand N, Xue SA, Larkin DF, Haskard DO, *et al*. Antibody targeted gene transfer to endothelium. J Gene Med. 2003;5:311–23.
38. Kalchenko V, Shivtiel S, Malina V, Lapid K, Haramati S, Lapidot T, *et al*. Use of lipophilic near-infrared dye in whole-body optical imaging of hematopoietic cell homing. J Biomed Opt. 2006;11(5):505–7.
39. Kreuter J. Influence of the surface properties on nanoparticle mediated transport of drugs to the brain. J Nanosci Nanotechnol. 2004;4:484–8.
40. Kreuter J, Shamenkov D, Petrov V, Ramge P, Cychutek K, Koch-Brandt C, *et al*. Apolipoprotein-mediated transport of nanoparticle-bound drugs across the blood–brain barrier. J Drug Target. 2002;10:317–25.
41. Chang J, Paillard A, Passirani C, Morille M, Benoit J-P, Betbeder D, *et al*. Transferrin adsorption onto PLGA nanoparticles governs their interaction with biological systems from blood circulation to brain cancer cells. Pharm Research. 2012;29(6):1495–505.
42. Elias DR, Poloukhtine A, Popik V, Tsourkas A. Effect of ligand density, receptor density, and nanoparticle size on cell targeting. Nanomed Nanotech Biol Med. 2012;9:194–201.
43. Zheng X, Cheung LS, Schroeder JA, Jiang L, Zohar Y. Cell receptor and surface ligand density effects on dynamic states of adhering circulating tumor cells. Lab Chip. 2011;11(20):3431–9.
44. Yuan H, Zhang S. Effects of particle size and ligand density on the kinetics of receptor-mediated endocytosis of nanoparticles. Appl Phys Lett. 2010;96(3):0337041–3.
45. Gunawan RC, Auguste DT. The role of antibody synergy and membrane fluidity in the vascular targeting of immunoliposomes. Biomaterials. 2010;31(5):900–7.
46. Srivastava RAK, Ito H, Hess M, Srivastava N, Schonfeld G. Regulation of low density lipoprotein receptor gene expression in HepG2 and Caco2 cells by palmitate, oleate, and 25-hydroxycholesterol. J Lipid Research. 1995;36:1434–46.
47. Keck CM, Jansch M, Müller RH. Protein adsorption patterns and analysis on IV Nanoemulsions—The key factor determining the organ distribution. Pharmaceutics. 2013;5:36–68.